SCIENCE CHINA
Information Sciences

• LETTER •

October 2017, Vol. 60 109301:1–109301:3
doi: 10.1007/s11432-016-0541-1

High-dynamics pulse-shaped signal simulation based on polynomial-based interpolation filters

Shaozhong LU, Yongqing WANG*, Sheng LI & Siliang WU

School of Information and Electronics, Beijing Institute of Technology, Beijing 100081, *China*

Received December 1, 2016; accepted December 29, 2016; published online February 20, 2017

Citation Lu S Z, Wang Y Q, Li S, et al. High-dynamics pulse-shaped signal simulation based on polynomial-based interpolation filters. Sci China Inf Sci, 2017, 60(10): 109301, doi: 10.1007/s11432-016-0541-1

Dear editor,

Baseband signal shaping is widely applied in satellite communication, GNSS, and TT&C systems as a fundamental technique [1]. These systems work in high-speed dynamic environments, causing data rate variations because of the Doppler effect, thus affecting the receivers' synchronization and measurement performances. To validate the performances of receivers at the testing stage, high-dynamics pulse-shaped signals must be simulated.

Pulse-shaped signals are generated using pulse-shaping filters (PSFs). For high-dynamic pulse-shaped signals, the PSF should be capable of handling time-varying sample rate conversion (SRC) ratios. The traditional finite/infinite impulse response (FIR/IIR), cascaded integrator-comb, and polyphase filters are thus not suitable [2]. Therefore, a real-time variable SRC structure, called polynomial-based interpolation filters [3–5], is applied. It can be implemented via the Farrow structure and its modifications, using the different design methods [4–6]. A fractional interval parameter is used to control the SRC ratio at any time. Herein, a high-dynamics pulse-shaped signal model is proposed based on the interpolation theory. A PSF is implemented via a modified Farrow structure using an improved window design method to improve performance and reduce complexity.

Signal model. According to the interpolation theory [3], the high-dynamics pulse-shaped signal model is given by

$$y_{\mathrm{d}}[k] = \sum_{i=-I}^{I-1} x[m_k - i]\, h_{\mathrm{PSF}}[(i+\mu_k)\, T_0], \tag{1}$$

where $x[n]$ is the data sequence, T_0 is the fixed data period, $h_{\mathrm{PSF}}(t)$ is the impulse response of PSF, $2I$ is the truncation length, m_k is the base-point index, μ_k is the fractional interval, and $i = m_k - n$. Parameters m_k and μ_k are defined as

$$m_k = \left\lfloor \sum_{n=0}^{k} (R_0 + R_{\mathrm{d}}[n])\, T_{\mathrm{s}} - \frac{d_0}{\mathrm{c}} R_0 \right\rfloor,$$
$$\mu_k = \sum_{n=0}^{k} (R_0 + R_{\mathrm{d}}[n])\, T_{\mathrm{s}} - \frac{d_0}{\mathrm{c}} R_0 - m_k, \tag{2}$$

where $\lfloor \cdot \rfloor$ is the floor operator, T_{s} is the sampling interval, c is the speed of light, d_0 is the initial satellite-to-earth distance at $t = 0$, $R_0 = 1/T_0$ is the data rate, and $R_{\mathrm{d}}[n]$ is the Doppler data rate. Eq. (2) shows the parameters m_k and μ_k can be calculated by a numerically controlled oscillator. Notice that $R_{\mathrm{d}}[n]$ is not the focus here, and we assume that $R_{\mathrm{d}}[n]$ has been accurately resolved [7].

Improved window design method. We improve the traditional window design method [4]. The windowed $h_{\mathrm{PSF}}(t)$ is denoted as $h(t)$, nonzero for $-IT_0 \leqslant t < IT_0$. $T = \gamma^{-1} T_0$ is defined as polynomial segment length, where γ is a positive integer.

* Corresponding author (email: wangyongqing@bit.edu.cn)
The authors declare that they have no conflict of interest.

Substituting $h(t)$ and $T = \gamma^{-1}T_0$ into (1) yields

$$y_{\mathrm{d}}[k] = \sum_{i=-I}^{I-1} x[m_k - i]\, h(\gamma i + i'_k, \mu'_k), \quad (3)$$

where $h(\gamma i + i'_k, \mu'_k) = h[(\gamma i + i'_k)T + \mu'_k T]$, $i'_k = \lfloor \gamma\mu_k \rfloor$, and $\mu'_k = \gamma\mu_k - i'_k$. The interval T_0 is divided into γ sub-intervals and $\mu_k T_0$ is expressed by parameters i'_k and μ'_k, where $i'_k = 0, 1, \ldots, \gamma-1$ is the index of the sub-interval and $\mu'_k T$, $0 \leqslant \mu'_k < 1$, is the fractional interval in this sub-interval.

According to the previous impulse response synthesis technique [5], the impulse response segments are approximated by N-order polynomials:

$$h(\gamma i + i'_k, \mu'_k) \approx \sum_{n=0}^{N} c_n(\gamma i + i'_k)(2\mu'_k - 1)^n, \quad (4)$$

where the coefficients follow the symmetry relation $c_n(\gamma i + i'_k) = (-1)^n c_n(-(\gamma i + i'_k) - 1)$. Therefore, the number of filter coefficients and multipliers can be reduced by half. The coefficients $c_n(\gamma i + i'_k)$ can be obtained from the coefficients $b_n(\gamma i + i'_k)$ of the traditional Farrow structure [6]:

$$c_n(\gamma i + i'_k) = \sum_{k=n}^{N} \frac{1}{2^k} \begin{pmatrix} k \\ n \end{pmatrix} b_k(\gamma i + i'_k). \quad (5)$$

We then use Lagrange interpolation to obtain the piecewise polynomial approximation. The coefficients $b_n(\gamma i + i'_k)$ can be solved by

$$\begin{aligned} &\boldsymbol{B} = \boldsymbol{H}\boldsymbol{A}, \quad \boldsymbol{B} = [b_n(\gamma i + i'_k)], \\ &\boldsymbol{H} = [h_n(\gamma i + i'_k)], \quad \boldsymbol{A} = [a_n(m)]^{\mathrm{T}}, \end{aligned} \quad (6)$$

where $h_n(\gamma i + i'_k) = h(\gamma i + i'_k, n/N)$, $\gamma i + i'_k$ and m are the row indices, n is the column index, and coefficients $a_n(m)$ in $\boldsymbol{A}$ can be obtained using

$$\sum_{m=0}^{N} a_n(m)\, {\mu'_k}^m = \prod_{j=0, j\neq n}^{N} \frac{\mu'_k N - j}{n - j}. \quad (7)$$

Modified Farrow structure. We modify the original Farrow structure considering the above design method. Substituting (4) into (3) yields

$$y_{\mathrm{d}}[k] \approx \sum_{n=0}^{N} v(n)\,(2\mu'_k - 1)^n, \quad (8a)$$

$$v(n) = \sum_{i=-I}^{I-1} x[m_k - i]\, c_n(\gamma i + i'_k), \quad (8b)$$

where $v(n)$ are parallel FIR filters, and the transfer functions are denoted as $C_n(z)$. In terms of (8a), the modified Farrow structure is shown in Figure 1(a); it consists of $N+1$ parallel FIR filters. The modifications are the parallel FIR filters' structure and the use of parameters i'_k and μ'_k.

Using the multiple sampling rate theory [8], Eq. (8b) can be regarded as the data sequence that is filtered by the i'_k-th polyphase component of the filter $C_n(z)$. Hence, the filter $C_n(z)$ can be implemented via the polyphase structure. The polyphase decomposition of $C_n(z)$ is defined as

$$C_n(z) = \sum_{i'_k=0}^{\gamma-1} C_{n,i'_k}(z^\gamma), \quad (9)$$

where $C_{n,i'_k}(z)$ is the transfer function of the i'_k-th polyphase components. Because $C_n(z)$ is an odd order symmetric or antisymmetric filter, $C_{n,\lfloor\gamma/2\rfloor}(z)$ (it exists only when γ is odd) is symmetric or antisymmetric when n is even or odd, and other polyphase components can be obtained as the sum and difference of $\lfloor\gamma/2\rfloor$ pairs of FIR filters, $E_{n,m}(z)$ and $F_{n,m}(z)$, given by [8]

$$\begin{aligned} E_{n,m}(z) &= [C_{n,m}(z) + C_{n,\gamma-1-m}(z)]/2, \\ F_{n,m}(z) &= [C_{n,m}(z) - C_{n,\gamma-1-m}(z)]/2, \end{aligned} \quad (10)$$

where $m = 0, 1, \ldots, \lfloor\gamma/2\rfloor - 1$. Filters $E_{n,m}(z)$ are symmetric or antisymmetric when n is even or odd, and filters $F_{n,m}(z)$ are antisymmetric or symmetric when n is even or odd.

The polyphase structure of filter $C_n(z)$ is illustrated in Figure 1(b). The difference between the polyphase structure in Figure 1(b) and the one in [8] is that the commutator only selects the output samples of the i'_k-th polyphase filter $C_{n,i'_k}(z)$ at input rate. Hence, only two subfilters, $E_{n,m}(z)$ and $F_{n,m}(z)$, operate during each calculation. Because the structures of all subfilters are the same, only one copy of the subfilters is needed; however, it operates at two times the input rate with coefficients $E_{n,m}(z)$ and $F_{n,m}(z)$, respectively.

Comparison and verification. We implement the PSF based on a polynomial-based interpolation filter using three design methods: least-mean-square synthesis (referred to as L_2) [5], traditional window design [4], and the proposed improved window design. The first two methods result in the modified Farrow structure proposed in [5]. The last method results in the proposed modified Farrow structure. We define the PSF as being a raised cosine roll-off filter with a roll-off factor of 0.5; the impulse response of the PSF is truncated with a Hamming window; the truncation length $2I = 32$.

Figure 1(c) shows the properties of the PSFs designed using different methods and parameters. δ_{p} and A_{s} denote the maximum passband deviation from unity on a linear scale and the minimum

Method	N	γ	$\delta_{\rm p}$	$A_{\rm s}$ (dB)	Number of multipliers	Number of adders	Number of coefficients
L_2	5	1	7.5×10^{-4}	78.2	102	192	96
Window	5	1	2.3×10^{-4}	62.0	102	192	96
Improved window	5	1	1.1×10^{-4}	76.4	102	198	96
Improved window	2	8	1.2×10^{-4}	78.3	51	99	384

(c)

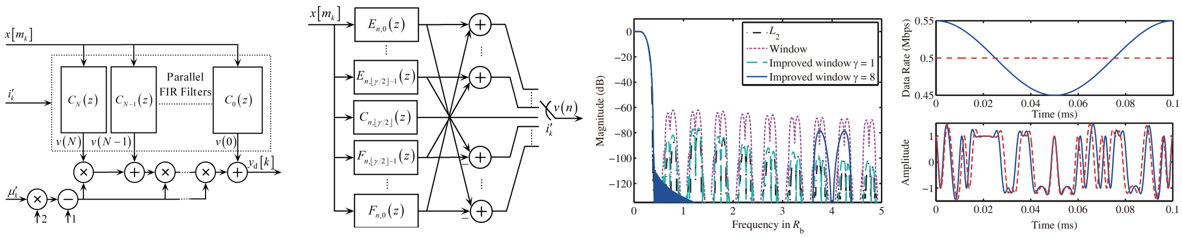

(a) (b) (d) (e)

Figure 1 (Color online) (a) Modified Farrow structure; (b) polyphase structure of the parallel FIR filter; (c) properties of the PSFs designed using different methods and parameters (d) comparison of magnitude responses of the PSF designed using different methods and parameters; (e) comparison of high-dynamic and non-dynamic pulse-shaped signals.

stopband attenuation in dB of the PSFs' magnitude response, respectively. The corresponding magnitude responses are compared in Figure 1(d). Under the same parameters, the frequency performance of the PSF designed using the proposed method is comparable to the one obtained with the L_2 synthesis technique, and the complexities of the proposed structure and the one proposed in [5] are almost the same. Under the same frequency performances, the proposed method and structure sacrifice the complexity of coefficients storage for the reduction of the complexities of multipliers and adders. It is useful in most cases of FPGA, because it has far less multiplier and adder resources than coefficients storage resource. Figure 1(e) shows the high-dynamics and non-dynamics data rates and the corresponding pulse-shaped signals. The data rate is $R_0 = 0.5$ Mbps, the Doppler data rate variation model is a cosine function, the maximum Doppler data rate $R_{\rm d\,max} = 0.05$ Mbps, and the Doppler data rate variation period is 0.1 ms. The high-dynamic pulse-shaped signal is generated using the proposed modified Farrow structure with the design parameters listed in the last line of Figure 1(c). Comparing these two signals, it is clear that the high-dynamics pulse-shaped signal varies in close accordance with the varying data rate. Therefore, the proposed method is capable of perfectly handling the time-varying SRC ratio condition, and accurately simulates the desired signals.

Conclusion. We have presented a high-dynamic pulse-shaped signal simulation method based on polynomial-based interpolation filters. The work illustrated a PSF implemented via a modified Farrow structure using an improved window design method and demonstrated that lower complexity and better performance could be obtained than other methods. The simulation results validated that the proposed simulation method is capable of handling the time-varying SRC ratio condition, and accurately simulates the desired signals.

Acknowledgements This work was supported by National Natural Science Foundation of China (Grant No. 61401026).

Supporting information The supporting information is available online at info.scichina.com and link.springer.com. The supporting materials are published as submitted, without typesetting or editing. The responsibility for scientific accuracy and content remains entirely with the authors.

References

1 Floch J J, Issler J L, Antreich F, et al. Comparison of different chip pulse shapes for DS-CDMA systems. In: Proceedings of IEEE/ION Position Location & Navigation Symposium, Indian Wells, 2010. 918–926
2 Mukumoto K, Wada T. Realization of root raised cosine roll-off filters using a recursive FIR filter structure. IEEE Trans Commun, 2014, 62: 2456–2464
3 Lamb D, Chamon L F O, Nascimento V H. Efficient filtering structure for spline interpolation and decimation. Electron Lett, 2016, 52: 39–41
4 Babic D. Windowing design method for polynomial-based interpolation filters. Circ Syst Signal Process, 2013, 32: 759–780
5 Vesma J, Saramäki T. Polynomial-based interpolation filters—Part I: Filter synthesis. Circ Syst Signal Process, 2007, 26: 115–146
6 Farrow C W. A continuously variable digital delay element. In: Proceedings of IEEE International Symposium on Circuits and Systems, Espoo, 1988. 2641–2645
7 Zhou Y, Zheng Z, Wu S L. A novel generalized simulation technology of aerospace TT&C channel. Chin J Electron, 2014, 23: 204–208
8 Johansson H, Göckler H. Two-stage-based polyphase structures for arbitrary-integer sampling rate conversion. IEEE Trans Circ Syst II Exp Briefs, 2015, 62: 486–490